Atmospheric
Chemistry
and Physics
Discussions

Open Access

# Middle atmospheric changes caused by the January and March 2012 solar proton events

C. H. Jackman[1], C. E. Randall[2], V. L. Harvey[2], S. Wang[3], E. L. Fleming[1,4],
M. López-Puertas[5], B. Funke[5], and P. F. Bernath[6,7]

[1]NASA Goddard Space Flight Center, Code 614, Greenbelt, MD, USA
[2]Laboratory for Atmospheric and Space Physics and Department of Atmospheric and Oceanic Sciences, University of Colorado, Boulder, CO, USA
[3]Jet Propulsion Laboratory, California Institute of Technology, Pasadena, CA, USA
[4]Science Systems and Applications, Inc., Lanham, MD, USA
[5]Instituto de-Astrofisica de Andalucia, CSIC, Granada, Spain
[6]Department of Chemistry and Biochemistry, Old Dominion University, Norfolk, VA, USA
[7]Department of Chemistry, University of York, York, UK

Title Page

| Abstract | Introduction |
| Conclusions | References |
| Tables | Figures |

|◄ | ►|
◄ | ►

Back | Close

Full Screen / Esc

Printer-friendly Version

Interactive Discussion

## Abstract

The recent 23–30 January and 7–11 March 2012 solar proton event (SPE) periods were substantial and caused significant impacts on the middle atmosphere. These were the two largest SPE periods of solar cycle 24 so far. The highly energetic solar
5　protons produced considerable ionization of the neutral atmosphere as well as $HO_x$ (H, OH, $HO_2$) and $NO_x$ (N, NO, $NO_2$). We compute a $NO_x$ production of 1.9 and 2.1 Gigamoles due to these SPE periods in January and March 2012, respectively, which places these SPE periods among the 12 largest in the past 50 yr. Aura Microwave Limb Sounder (MLS) observations of the peroxy radical, $HO_2$, show significant enhance-
10　ments of $> 0.9$ ppbv in the northern polar mesosphere as a result of these SPE periods. Both MLS measurements and Goddard Space Flight Center (GSFC) two-dimensional (2-D) model predictions indicated middle mesospheric ozone decreases of $> 20$ % for several days in the northern polar region with maximum depletions $> 60$ % over 1–2 days as a result of the $HO_x$ produced in both the January and March 2012 SPE peri-
15　ods. The SCISAT-1 Atmospheric Chemistry Experiment Fourier Transform Spectrometer (ACE) and the Envisat Michelson Interferometer for Passive Atmospheric Sounding (MIPAS) instruments measured NO and $NO_2$ ($\sim NO_x$), which indicated enhancements of over 20 ppbv in most of the northern polar mesosphere for several days as a result of these SPE periods. The GSFC 2-D model was used to predict the medium-
20　term ($\sim$ months) influence and showed that the polar middle atmosphere ozone was most affected by these solar events in the Southern Hemisphere due to the increased downward motion in the fall and early winter. The downward transport moved the SPE-produced $NO_y$ to lower altitudes and led to predicted modest destruction of ozone (5–9 %) in the upper stratosphere days to weeks after the March 2012 event. Total ozone
25　reductions were predicted to be a maximum of 1 % in 2012 due to these SPEs.

Title Page

| Abstract | Introduction |
| Conclusions | References |
| Tables | Figures |

|◀ ▶|

◀ ▶

Back Close

Full Screen / Esc

Printer-friendly Version

Interactive Discussion

# 1   Introduction

Solar flares erupted in January and March 2012 and sent large fluxes of charged particles towards the Earth. Much of the energy was carried by solar protons, which impacted the middle atmosphere (stratosphere and mesosphere) leading to ioniza-
tions, dissociations, dissociative ionizations, and excitations. Such periods are generally known as solar proton events (SPEs) and cause proton-induced atmospheric interactions resulting in the production of $HO_x$ (H, OH, $HO_2$), and $NO_x$ (N, NO, $NO_2$) constituents either directly or through a photochemical sequence in the polar middle atmosphere. Such $HO_x$ and $NO_x$ enhancements can then lead to a perturbation of ozone.

The major influence of these eruptions caused enhanced solar proton flux levels above background at the Earth for several days in January and March 2012. Although SPEs and their middle atmospheric constituent influences have been studied before (e.g., Swider and Keneshea, 1973; Heath et al., 1977; Solomon et al., 1981; McPeters and Jackman, 1985; Randall et al., 2001; López-Puertas et al., 2005a; von Clarmann et al., 2005; Verronen et al., 2006; Krivolutsky et al., 2006; Funke et al., 2011; Jackman et al., 2007, 2008, 2009, 2011; Sinnhuber et al., 2012), each new event offers a chance to investigate the SPE-caused atmospheric perturbation under somewhat different conditions. Also, such events have been shown to cause some longer lasting stratospheric changes (e.g., Randall et al., 2001; Jackman et al., 2008, 2009) and need to be considered within the context of other ongoing stratospheric changes (WMO, 2011).

The recent study of von Clarmann et al. (2013) showed several atmospheric constituent changes due to the January and March 2012 SPEs using Envisat Michelson Interferometer for Passive Atmospheric Sounding (MIPAS) instrument measurements. These latest large events, which provided very significant middle atmospheric impulses over short (∼ days) periods of time, also offer new opportunities to test the general understanding of an atmospheric change caused by very substantial perturbations.

For example, the January 2012 SPE period occurred in the Northern Hemisphere (NH) winter and Southern Hemisphere (SH) summer. The solar zenith angle (SZA) was very different in the NH and SH polar regions for this month of the year. Since the SZA dramatically impacts the background atmosphere upon which the SPE-caused perturbation interacts, the ultimate SPE-caused atmospheric variation is highly dependent on the SZA. The influences of the SPE-produced $HO_x$ and $NO_x$ species impacted ozone somewhat differently in the two hemispheres in January. Also, the NH was subject to a sudden stratospheric warming (SSW) event along with a mesospheric cooling in January (see von Clarmann et al., 2013).

The March 2012 SPE period occurred closer to equinox for the two hemispheres, however, the NH was transitioning to spring and the SH was transitioning to fall. This meant that the SPE-caused $NO_x$ was transported somewhat differently in the two hemispheres and had a larger impact on ozone in the SH than in the NH.

We will show the measured influence of these SPEs on $HO_2$ and ozone from the Aura Microwave Limb Sounder (MLS) instrument. The influence of these SPEs on the sum of NO and $NO_2$ ($\sim NO_x$) from the SCISAT-1 Atmospheric Chemistry Experiment Fourier Transform Spectrometer (ACE-FTS) and the Envisat MIPAS instruments will also be shown. These observations of the atmospheric response to the January and March 2012 SPE periods will be compared with global model predictions.

This paper is divided into seven primary sections, including the Introduction. The solar proton flux and ionization rate computation are discussed in Sect. 2 and SPE-induced production of $HO_x$ and $NO_x$ are discussed in Sect. 3. A description of the Goddard Space Flight Center (GSFC) two-dimensional (2-D) model is given in Sect. 4. GSFC 2-D model results for short-term (days) $HO_2$, ozone, and $NO_x$ constituent changes, with comparisons to measurements for these SPEs, are shown in Sect. 5 while medium-term (months) constituent changes caused by these SPEs are discussed in Sect. 6. The conclusions are presented in Sect. 7.

## 2 Proton flux and ionization rate

We use the solar proton flux (energies 1 to 300 MeV) provided by the National Oceanic and Atmospheric Administration (NOAA) Space Weather Prediction Center (SWPC) for the NOAA Geostationary Operational Environmental Satellites (GOES) (see http: //www.swpc.noaa.gov/ftpmenu/lists/particle.html). The GOES 13 data are considered to be the most reliable of the current GOES datasets for the proton fluxes depositing energy into polar latitudes and were used as the source of protons in several energy intervals for the very active time periods 23–30 January 2012 and 7–11 March 2012. For example, the GOES proton flux during the 22–30 January 2012 time period is given in Fig. 1 for several different energies (> 1, > 10, > 30, > 50, and > 100 MeV). Note that the proton flux levels increased by a factor of a thousand or more for energies > 10, > 30, and > 50 MeV on 23 January 2012. Four days later (27 January) another event led to proton flux levels increasing by a factor of more than a hundred for > 30, > 50, and > 100 MeV.

The proton flux data were used to compute the ion pair production profiles employing the energy deposition methodology discussed in Jackman et al. (1980), where the creation of one ion pair was assumed to require 35 eV (Porter et al., 1976). The SPE-produced daily average ionization rates for the polar cap regions (> 60° geomagnetic latitude) are given in Fig. 2 for a nine day period in January 2012 from 10 hPa (∼ 30 km) to 0.001 hPa (∼ 95 km). Peak ionization rates above 2000 cm$^{-3}$ s$^{-1}$ on 24 January were computed for the 0.01 to 0.2 hPa region. The ionization was greatly diminished by 26 January, but then the second SPE started late on 27 January and reached a peak on 28 January (also, see Fig. 1).

The GOES proton flux during the 6–11 March 2012 time period is given in Fig. 3 for the same proton energies as in Fig. 1. The proton flux levels increased by a factor of a thousand or more for several energies (from > 10 through > 100 MeV) on 7–8 March 2012. The SPE-produced daily average ionization rates during this event for the polar cap regions are given in Fig. 4. Peak ionization rates above 2000 cm$^{-3}$ s$^{-1}$ on 8 March

were computed for the 0.01 to 0.3 hPa region. Large ionization rates $> 100\,\text{cm}^{-3}\,\text{s}^{-1}$ are computed all the way down to 10 hPa on 7–8 March. As illustrated in Fig. 3 compared with Fig. 1, this SPE period consisted of a larger flux of protons at higher energies ($> 100$ MeV) than were present in the January 2012 SPE period. The ionization is greatly diminished by 11 March.

## 3   $HO_x$ (H, OH, $HO_2$) and $NO_x$ (N, NO, $NO_2$) production

Charged particle precipitation results in the production of $HO_x$ through complex positive ion chemistry (Solomon et al., 1981). The charged particle-produced $HO_x$ is a function of ion pair production and altitude and is included in model simulations using a lookup table from Jackman et al. (2005, Table 1), which is based on the work of Solomon et al. (1981). Each ion pair results in the production of about two $HO_x$ constituents for the upper stratosphere and lower mesosphere and less than two $HO_x$ constituents for the middle and upper mesosphere.

  $NO_x$ is produced when the energetic charged particles (protons and associated secondary electrons) dissociate $N_2$ as they precipitate into the atmosphere. Here it is assumed that $\sim 1.25$ N atoms are produced per ion pair and the proton impact of N atom production is divided between the ground state $N(^4S)$ ($\sim 45\,\%$ or $\sim 0.55$ per ion pair) and excited state $N(^2D)$ ($\sim 55\,\%$ or $\sim 0.7$ per ion pair) nitrogen atoms (Porter et al., 1976). We calculate that the 23–30 January 2012 SPE period produced about 1.9 Gigamoles of $NO_x$ and that the 7–11 March 2012 SPE period produced about 2.1 Gigamoles of $NO_x$. Thus, the January 2012 and the March 2012 SPE periods were computed to be the twelfth and tenth largest in the past 50 yr, respectively (see Jackman et al., 2008).

## 4   Model predictions

### 4.1   Model description

The latest version of the Goddard Space Flight Center (GSFC) two-dimensional (2-D) atmospheric model was used to predict the impact of solar protons on the atmosphere. This model was first discussed over 20 yr ago (Douglass et al., 1989; Jackman et al., 1990) and has undergone extensive improvements over the years (e.g., Considine et al., 1994; Jackman et al., 1996; Fleming et al., 1999, 2007, 2011). The vertical range of the model, equally spaced in log pressure, is from the ground to approximately 92 km (0.0024 hPa) with a 1 km grid spacing. The model has a 4° latitude grid spacing.

The transport is derived using the daily average global winds and temperatures from the NASA Modern Era Retrospective-analysis for Research and Applications (MERRA) meteorological analysis (see the website: http://gmao.gsfc.nasa.gov/research/merra/) for 1979–2010. Thirty-day running averages of the residual circulation, eddy diffusion, zonal mean wind, and zonal mean temperature are computed using the methodology detailed in Fleming et al. (2007). For this paper we constructed a climatological average of the transport over these years and applied it over the simulated periods. The averaged transport fields change daily, but repeat yearly.

The ground boundary conditions in the GSFC 2-D model for the source gases are taken from WMO (2011) for year 2012. The model uses a chemical solver described in Jackman et al. (2005) and Fleming et al. (2007, 2011). The photochemical gas and heterogeneous reaction rates and photolysis cross sections have been updated to the latest Jet Propulsion Laboratory recommendations (Sander et al., 2010) for these computations.

### 4.2   Model simulations

The starting conditions for the two GSFC 2-D model simulations used in this study were provided by a time dependent "spin-up" simulation from January 2000–December

2011, which included the appropriate source gas boundary conditions from WMO (2011). Two time-dependent simulations, "A" and "B", were continued over the period 1 January through 31 December 2012. Simulation "A" included no SPEs and simulation "B" included all SPEs in this period.

## 5   Short-term Influences of the SPEs

A number of constituents have been observed and modeled to be modified by SPEs (e.g., López-Puertas et al., 2005a, b; von Clarmann et al., 2005; Verronen et al., 2006; Jackman et al., 2011; Damiani et al., 2012). We will focus on the SPE-caused impact on $HO_x$, $NO_x$, and ozone in this study. The SPEs can cause substantial increases in $HO_x$ and $NO_x$ constituents (see Sect. 3), which can directly impact ozone through catalytic destruction cycles (e.g., see Johnston and Podolske, 1978).

### 5.1   Peroxy radical ($HO_2$)

The Aura Microwave Limb Sounder (MLS) measurement of the peroxy radical ($HO_2$) provides a direct observation and quantification of $HO_x$ changes due to the January 2012 SPE in the middle atmosphere. Figure 5 (Top) shows the daily average MLS $HO_2$ changes from a five-day (18–22 January) average of $HO_2$ measurements before the SPE period for the 60–82.5° N band. Enhancements of $> 0.2$ ppbv are observed in the middle mesosphere over periods 23–26 January and 28–29 January. A peak of $> 1$ ppbv is observed from $\sim 0.05$–0.1 hPa on 24 January. These $HO_2$ enhancements are slightly larger than those reported in Jackman et al. (2011) for the January 2005 SPEs.

The measurement of $HO_2$ in the atmosphere by MLS is impressive given its relatively small relative abundance throughout the middle atmosphere, however, some care must be exercised in using these data. For example, MLS $HO_2$ has a bias that is usually removed by taking day-night differences over the entire recommended pressure

Title Page

Abstract | Introduction

Conclusions | References

Tables | Figures

◄ | ►

◄ | ►

Back | Close

Full Screen / Esc

Printer-friendly Version

Interactive Discussion

range. It was advantageous in this work to include all the MLS $HO_2$ measurements to determine the SPE-caused impact. Removal of the five-day average before the SPE period, as done in this study, will also lead to a removal of the MLS $HO_2$ bias assuming that the bias varies in only a minor way over a couple of weeks. Although the MLS $HO_2$ measurements are not recommended for scientific use above 0.046 hPa, those MLS observations are shown here to qualitatively indicate the morphology of the $HO_2$ change during the disturbed periods.

We also show the daily average MLS $HO_2$ changes from a five-day (18–22 January) average of $HO_2$ measurements before the SPE period for the 60–82.5° S band in Fig. 6 (Top). Note that the observed SH $HO_2$ enhancement is at a peak value of $> 0.5$ ppbv for the $\sim 0.015$–0.07 hPa region on 24 January, which is less than the peak levels shown in the NH (see Fig. 5). The $HO_x$ produced by the SPE is approximately the same in both hemispheres, however, the lifetime of $HO_2$ is diminished in the SH (summer) due to the higher background $HO_x$ level and a faster loss of $HO_2$ at this time of year. The increased solar radiation in the SH (summer) leads to an increase in the amount of mesospheric $HO_x$ by a factor of about 2–6 relative to the NH (see Fig. 7, GSFC 2-D model computations), thus the loss of $HO_2$ is larger in the SH through the increase in the rate of reactions

$$OH + HO_2 \rightarrow H_2O + O_2 \tag{R1}$$

and

$$H + HO_2 \rightarrow products \tag{R2}$$

The predicted $HO_2$ change from the five-day (18–22 January) average using simulation "B" is shown in Figs. 5 and 6 (Bottom) for the same period. Also, the MLS averaging kernel (AK) is applied to the model results. The variation with time and pressure as well as the magnitude of the computed change is fairly similar to the MLS $HO_2$ observations, especially in the NH. The predicted $HO_2$ increase is slightly smaller than the observed increase due to the SPEs in the SH, however, the pressure levels impacted are fairly

Title Page

Abstract | Introduction

Conclusions | References

Tables | Figures

|◀ | ▶|

◀ | ▶

Back | Close

Full Screen / Esc

Printer-friendly Version

Interactive Discussion

similar between the model and measured values. The predicted $HO_2$ enhancements due to the SPEs are within the computed precision error ($\sim 0.4$ ppbv near 0.1 hPa) for daily average MLS measurements of $HO_2$ in these latitude bands.

We also completed a similar analysis of the $HO_2$ enhancements caused by the March 2012 SPEs. The $HO_2$ changes from a five-day (2–6 March) average of $HO_2$ measurements before the SPE period for the 60–82.5° N and 60–82.5° S bands were examined. We found MLS observed enhancements of $> 0.2$ ppbv in the mesosphere over five days (7–11 March) with a peak of 0.8 ppbv occurring near 0.05 hPa on 8 March in the NH and observed enhancements $> 0.2$ ppbv on three days (7, 8, and 10 March) and a peak of 0.4 ppbv occurring near 0.05 hPa on 8 March in the SH (not shown).

The general location of the peaks and variations with pressure are fairly similar between the measurements and model predictions for $HO_2$ in early March 2012 during the SPE, however, there are some differences in the peak values. The predicted $HO_2$ change as a result of the March 2012 SPE shows a peak on 8 March near 0.02 to 0.05 hPa of about 1 ppbv for latitude band 60–82.5° N and a peak of about 0.7 ppbv for latitude band 60–82.5° S. Although the solar radiation is similar in the SH and NH polar regions in March, the level of $H_2O$, the ultimate source of $HO_x$, is somewhat different. More mesospheric SH $H_2O$ is predicted in March due to the upward motion during the Southern polar summer transporting up $H_2O$ from the upper stratospheric water source. Conversely, less mesospheric NH $H_2O$ is predicted in March due to downward motion during the Northern polar winter transporting down low amounts of $H_2O$ from the dry lower thermosphere. The larger amounts of polar SH $H_2O$ result in a larger predicted SH $HO_2$ peak during the SPE, compared with the polar NH.

## 5.2 Ozone

The $HO_x$ constituents are the primary cause of ozone depletion in the mesosphere during SPEs and the impact during the January and March 2012 SPE periods is seen clearly in the MLS ozone measurements. Several catalytic $HO_x$ cycles are important in

the middle atmosphere, however, the process

$$H + O_3 \rightarrow OH + O_2 \tag{R3}$$

followed by

$$OH + O \rightarrow H + O_2 \tag{R4}$$

5

$$\text{Net}: \ O + O_3 \rightarrow 2O_2 \tag{R5}$$

is dominant throughout much of the mesosphere. During strong SPEs, such as these in 2012, the $HO_x$ catalytic cycle

$$OH + O_3 \rightarrow HO_2 + O_2 \tag{R6}$$

10  followed by

$$HO_2 + O \rightarrow OH + O_2 \tag{R7}$$

$$\text{Net}: \ O + O_3 \rightarrow 2O_2 \tag{R8}$$
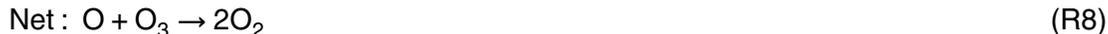
also contributes significantly to the ozone decrease.

15  We show the MLS daily average ozone change from a five-day (18–22 January) average of ozone measurements before the SPE period for the 60–82.5° N band in Fig. 8 (Top). Ozone depletions of $> 20\%$ are observed in the middle mesosphere for the 60–82.5° N band over the 24–27 January period with a maximum of 60 % depletion occurring near 0.02–0.05 hPa on 25 January (Fig. 8, Top). The $HO_x$ constituents have

20  a relatively short lifetime ($\sim$ hours) throughout most of the mesosphere (below $\sim$ 80 km,

Full Screen / Esc

Printer-friendly Version

Interactive Discussion

see Pickett et al., 2006), however, they can cause very large ozone depletion, which has also been observed in other very large substantial SPEs (e.g., Solomon et al., 1983; Jackman et al., 2001, 2011; Verronen et al., 2006).

Surprisingly, the MLS observations show an increase in ozone at their retrieval level of 0.046 hPa for 28–30 January, with ozone decreases above and below. It is unclear what causes this MLS-observed ozone increase at the 0.046 hPa level during this period. MIPAS ozone measurements at this same time period and location do not appear to show this behavior (von Clarmann et al., 2013). The observed ozone increases at pressures greater than 0.5 hPa are caused by seasonal changes ongoing at this time of year, which mitigate and overwhelm the SPE-caused ozone decrease.

We show two model computations of the SPE-caused predicted ozone change in Fig. 8 (Middle and Bottom). The model predicted changes in Fig. 8 (Middle) are derived in the same manner as the MLS observed changes, wherein the modeled ozone in simulation "B" is subtracted from the five-day (18-22 January) average of modeled ozone before the SPE period. Thus, this model predicted change will also have seasonal variations included. The model predicted changes for Fig. 8 (Bottom) are derived by subtracting simulation "A" from simulation "B" to produce a SPE-only caused ozone change thereby removing the seasonal ozone increase in the upper stratosphere. As in Figs. 5 and 6, the MLS averaging kernel (AK) is applied to the model results. Note that there are some differences between the measurements and model predictions (see Fig. 8, Top and Middle). For example, although both the measurements and model predictions indicate a SPE-caused ozone depletion in the middle mesosphere over the 24–27 January period, the model predicts a somewhat larger altitude range of predicted ozone decrease from the SPEs as well as a smaller seasonal increase in the upper stratosphere and lower mesosphere.

As in Fig. 8 (Top), we show the MLS daily average ozone change from a five-day (18–22 January) average of ozone measurements before the SPE period for the 60-82.5° S band in Fig. 9 (Top). Ozone depletions of > 10 % are observed in the middle mesosphere for the 60–82.5° S band over the 23–24 January period with a maximum

of 30 % depletion occurring near 0.02 hPa on 23 January. A small depletion from about 2–0.04 hPa is even observed on 28 January as a result of the second SPE in January. These SPE-caused ozone depletions are less in the polar SH due to the shorter lifetime of $HO_x$ (and ultimate $HO_x$ influence) in the summer relative to the winter (e.g., see

5  Solomon et al., 1983; Jackman et al., 2008).

We show two computations of the SPE-caused predicted ozone change for the 60–82.5° S band in Fig. 9 (Middle and Bottom), derived in the same way as the model predictions in Fig. 8. The model predicted ozone change is in generally reasonable agreement with the observed MLS ozone changes on 23–24 January, both in the mag-

10  nitude and timing. The model predicted changes shown in Fig. 9 (Bottom), derived by subtracting simulation "A" from "B", indicate that seasonal increases in ozone are important in the upper stratosphere ($\sim$ 1–6 hPa).

Given the somewhat surprising MLS observations of an increase in ozone at the retrieval level of 0.046 hPa in the 60–82.5° N band for the SPE on 28–30 January (see

15  Fig. 8, Top), we show the MLS observations during the March 2012 SPE period for this same region in Fig. 10 (Top). Clearly, MLS measured mesospheric ozone is being depleted at all levels as a result of the SPE. The model results given in Fig. 10 (Middle, Bottom), computed in the same way as in Figs. 8 and 9, also show ozone being depleted throughout the mesosphere. Both measurements and model results show

20  ozone decreases > 60 % on 8–9 March at about 0.05–0.02 hPa. The measurements and model simulations also indicate a modest seasonally-driven ozone increase in the upper stratosphere. As an aside, MIPAS observations show similar ozone depletion due to the March 2012 SPE.

We also examined the MLS ozone observations as well as our model predictions

25  for the 60–82.5° S band during the March 2012 SPE period (not shown). The measurements and model results indicate significant ozone depletion as a result of the SPE with both showing ozone decreases > 20 % on 8 March through the middle mesosphere. The model predictions do indicate a somewhat larger ozone depletion for the 7–11 March period, when compared to the MLS measurements.

**Atmospheric changes from solar proton events in 2012**

C. H. Jackman et al.

Title Page

Abstract | Introduction

Conclusions | References

Tables | Figures

⏮ | ⏭

◀ | ▶

Back | Close

Full Screen / Esc

Printer-friendly Version

Interactive Discussion

## 5.3 Nitrogen oxides, $NO_x$ ($NO+NO_2$)

ACE-FTS (hereinafter referred to as ACE) (Bernath et al., 2005) and MIPAS (Fischer et al., 2008) measured both NO and $NO_2$ (e.g., Rinsland et al., 2005; López-Puertas et al., 2005a). We defined $NO_x$ in Sect. 1 as $N + NO + NO_2$, but here we identify $NO_x$
5  as approximated by $NO + NO_2$ since N is minuscule in the middle atmosphere.

ACE provided $NO + NO_2$ profile measurements at fairly high latitudes during the January through April 2012 period. For example, for the period Days of Year (DoY) 22–47 (22 January to 16 February) ACE observations were made in the NH between about 65 and 68° N. The ACE measured $NO_x$ changes from DoY 22 (22 January) are shown
10  in Fig. 11a. Large increases (> 100 ppbv) are observed in the middle to upper mesosphere (< 0.05 hPa) for DoY 24–36. Some of these increases are certainly due to the solar protons and associated secondary electrons, however, energetic electron precipitation (EEP) may also be contributing in the middle and upper mesosphere (pressures < 0.1 hPa). The solar protons penetrate deeper into the atmosphere than the EEP, and
15  cause most of the measured enhanced $NO_x$ in the lower mesosphere.

Substantial increases (> 20 ppbv) were observed throughout most of the mesosphere for these same days continuing through Day of Year 44 for the lower mesosphere ($\sim$ 0.04–0.7 hPa). MIPAS measurements are also available during this time period, but not for every day, and are given in Fig. 11b. It should be noted that the MIPAS nominal
20  observations used here are limited to tangent heights of 70 km. Hence, the retrieved $NO_x$ profiles have little-to-no vertical resolution above 70 km. In the SH, MIPAS $NO_x$ might be underestimated (due to the effect of the a priori profile shape) even down to 65 km.

In spite of these important caveats, the MIPAS measurements are generally in agree-
25  ment with ACE when the slightly larger averaging kernels of MIPAS are taken into account. Such measured $NO_x$ enhancements were similar to those observed by ACE as a result of the January 2005 SPEs (Jackman et al., 2011).

ACE also takes measurements at high southern latitudes, however, the number of days of observations is relatively limited and will not be shown. A comparison of the SPE-caused $NO_x$ enhancement over a larger polar region (60–90°) is shown in Figs. 12 and 13 for the NH and SH, respectively, for the MIPAS instrument (Top plots) and the GSFC 2-D model (Bottom plots). The model indicates a somewhat smaller $NO_x$ change in the NH and a somewhat larger $NO_x$ change in the SH, compared with MIPAS observations. The smaller predicted $NO_x$ change in the NH may be related to the absence of concurrent energetic electron precipitation in our computations.

We turn our attention to the March 2012 SPE period in Fig. 14. The ACE and MIPAS measured $NO_x$ ppbv change from 6 March is shown in Fig. 14a, b and indicates enhancements of over 20 ppbv throughout most of the northern polar mesosphere for several days (DoY 68–74 for ACE and DoY 68–72 for MIPAS) as a result of this SPE period. Peak $NO_x$ increases over 100 ppbv were observed by ACE on DoY 68 (8 March) between 0.01 and 0.02 hPa as a result of the March 2012 SPE.

As during the January 2012 SPE period, ACE also takes measurements at high southern latitudes. Again, however, the number of days of observations is relatively limited and will not be shown. A comparison of the SPE-caused $NO_x$ enhancement over a larger polar region (60–90°) is shown in Figs. 15 and 16 for the NH and SH, respectively, for the MIPAS instrument (Top plots) and the GSFC 2-D model (Bottom plots). Although the impacted altitudes are similar between the measurements and the model predictions, the model indicates a somewhat larger $NO_x$ change in both hemispheres, when compared with MIPAS observations. Some of this larger model predicted SPE-caused $NO_y$ enhancement can be explained by the finer vertical grid of the model (1–2 km in the mesosphere) compared to the MIPAS vertical field of view of about 3 km (López-Puertas et al., 2005a).

The initial model predicted $NO_x$ enhancement is substantially larger than the measured enhancements, with peak increases greater than 100 ppbv on DoY 68–69 in the upper mesosphere for both hemispheres, compared with peak MIPAS measured increases of only about 40 ppbv (Figs. 15 and 16). Note also that the model predicted

$NO_x$ changes in the NH on DoY 76–80 show $> 5$ ppbv throughout most of the mesosphere (pressures $< 0.5$ hPa) whereas the MIPAS measured $NO_x$ changes are $< 5$ ppbv in the same region (Fig. 15). MIPAS measured mesospheric $NO_x$ enhancements are gone by DoY 81, however, model predicted $NO_x$ increases continue and gradually diminish in the lower mesosphere through DoY 97. The disappearance of NH MIPAS $NO_x$ enhancements is possibly related to a polar vortex rupture and release of $NO_x$ towards mid latitudes, which appears in MIPAS $CH_4$ data (not shown). Thus, there appear to be dynamical differences between the atmosphere and that simulated in the model. The model likely underestimates the amount of high latitude $NO_x$ transported to lower latitudes.

The model predicted $NO_x$ changes in the SH on DoY 76–80 are $\sim 5$–20 ppbv throughout the middle to lower mesosphere ($\sim 0.03$–0.7 hPa), which are in reasonable agreement with the MIPAS measurements during this time period (Fig. 16). In the upper stratosphere ($\sim 1$–3 hPa) slightly more SPE-produced $NO_x$ is simulated in the model than observed. Thus, the model predicts a slightly more substantial SPE-caused $NO_x$ perturbation in the SH, than indicated in the measurements; which will then cause a larger impact on stratospheric ozone.

Overall the model predicted $NO_x$ enhancements are larger than the MIPAS observations in both hemispheres for the March 2012 SPE. The proton flux source for the March 2012 SPE is the same as that for the January 2012 SPE (GOES 13), thus this $NO_x$ over-prediction is somewhat puzzling. Further model-measurement comparisons of these SPE-caused impacts will be needed to help understand this disagreement.

## 6 Medium-term Influences of the SPEs: odd nitrogen ($NO_y$) and ozone changes

The last three figures (Figs. 17–19) show only GSFC 2-D model predicted medium-term ($\sim$ months) influences of the SPE for all of 2012. These plots were derived by subtracting simulation "A" from simulation "B" to produce a SPE-only caused impact.

The NO$_x$ family rapidly converts in the stratosphere to other constituents in the odd nitrogen group (NO$_y$ = N($^4$S) + N($^2$D) + NO + NO$_2$ + NO$_3$ + 2N$_2$O$_5$ + HNO$_3$ + HO$_2$NO$_2$ + ClONO$_2$ + BrONO$_2$). The SPE-caused NO$_y$ and ozone percentage changes are given in Figs. 17 and 18 for the polar (60–90°) NH and SH, respectively. NO$_y$ enhancements exceeding 100 % are computed in the polar NH for most of the first five months of the year (J-F-M-A-M) throughout most of the mesosphere (Fig. 17, Top). In the upper stratosphere NO$_y$ is enhanced by up to about 50 %, however, the increases diminish greatly by August. The large computed NH ozone decreases (> 20 %, blue colors) during and shortly after the two SPE periods (January and March) were primarily caused by the SPE-produced HO$_x$ increases whereas the modest predicted ozone decreases of 1–5 % at lower levels were primarily caused by the SPE-produced NO$_y$ enhancements (Fig. 17, Bottom). The primary catalytic cycle for NO$_y$ destruction of ozone is:

$$NO + O_3 \rightarrow NO_2 + O_2 \tag{R9}$$

followed by

$$NO_2 + O \rightarrow NO + O_2 \tag{R10}$$

$$Net: \ O + O_3 \rightarrow 2O_2. \tag{R11}$$

The computed January–February NO$_y$ enhancements are not as substantial in the polar SH as in the polar NH due to considerable loss of odd nitrogen in the intense sunlight of SH summer and early fall. The reactions most important for this loss are:

$$NO + h\nu(< 191\,nm) \rightarrow N + O \tag{R12}$$

followed by

$$N + NO \rightarrow N_2 + O. \tag{R13}$$

C. H. Jackman et al.

Title Page

| Abstract | Introduction |
| Conclusions | References |
| Tables | Figures |

|◄ | ►|

◄ | ►

| Back | Close |

Full Screen / Esc

Printer-friendly Version

Interactive Discussion

The winds are also generally upwards in the SH in January and February, thus $NO_y$ constituents are transported upwards to the higher altitudes, where the loss process is greater. The vertical wind direction starts to reverse direction in early March and by late March is basically downwards (Fig. 18, Top). The wind reversal drags much more $NO_y$ from the mesosphere to the upper stratosphere by late May (Fig. 18, Top) leading to $NO_y$ enhancements $> 20\,\%$ (Fig. 18, Top) and associated ozone depletion of 5–9 % (Fig. 18, Bottom). $NO_y$ enhancements of $> 2\,\%$ and the associated ozone decreases of $> 1\,\%$ descend through the winter and spring, reaching 45 hPa by November. The predicted ozone depletion in the SH can be thought of as an "upper limit" given that the predicted SPE-caused $NO_x$ increases were somewhat higher than the measured SPE-caused $NO_x$ increases (see Fig. 16). Note, also, that there were other SPE periods in May, June, July, September, October, November, and December, which are seen in the enhanced $NO_y$ in both hemispheres (Figs. 17 and 18, Top panels). These particular SPE periods were not as large as those that occurred in January and March.

The impact of the 2012 SPEs on total ozone is shown in Fig. 19. Total ozone is reduced by a maximum of about 1 % approximately seven months after the March 2012 SPE period at the highest SH latitudes. The maximum total ozone changes are not predicted to occur during the SPE periods when the $HO_x$ catalytic cycles dominate; rather, the transport of the enhanced $NO_y$ to lower altitudes (and high ambient ozone amounts) causes more total ozone impact. Total ozone reductions $> 0.4\,\%$ are predicted to persist for several months (April–November) at high southern latitudes ($> 60°$). Total ozone reductions in the NH are predicted to be less than 0.2 %. Thus the impact of these SPE periods on total ozone is fairly small and it is unlikely that the perturbation could be detected in total ozone satellite or ground measurements.

# 7   Conclusions

The January and March 2012 SPE periods caused substantial perturbations to the Earth's middle atmosphere. In particular, measurements and global model predictions

showed impacts on mesospheric $HO_x$, $NO_x$, and ozone. MLS observations of $HO_2$ displayed enhancements up to 1 ppbv due to the January 2012 SPE period and up to 0.8 ppbv due to the March 2012 SPE period in the northern polar mesosphere. The southern polar mesosphere was impacted as well during these SPE periods, however,

5    the increased solar radiation (and enhanced $HO_x$ loss) impeded the $HO_2$ increase in January. The SPE-caused $HO_2$ enhancements were fairly well simulated with the GSFC 2-D model. Both MLS measurements and GSFC 2-D model predictions indicated middle mesospheric ozone decreases of > 20 % for several days in the northern polar region with maximum depletions > 60 % as a result of both the January and March

10   2012 SPE periods. Less SPE-caused ozone depletion was observed and simulated in the southern polar region in January 2012 due to the SPEs. Most of this mesospheric ozone depletion is the result of $HO_x$ catalytic loss cycles.

Both ACE and MIPAS measurements showed large SPE-caused $NO_x$ enhancements (> 20 ppbv) in the northern polar mesosphere for about three weeks past the January

15   2012 SPE period. The southern polar mesosphere MIPAS observations indicated a smaller SPE-caused $NO_x$ increase (< 20 ppbv) as a result of this January 2012 SPE period. The March 2012 SPE period caused $NO_x$ measured enhancements > 20 ppbv and > 10 ppbv for only several days in the northern and southern polar mesosphere, respectively. The GSFC 2-D model predicted $NO_x$ increases were slightly smaller (larger)

20   than measured in the northern (southern) polar mesosphere as a result of the January 2012 SPE period. The GSFC 2-D model predicted $NO_x$ enhancements as a result of the March 2012 SPE period were larger than observed in both polar hemispheres as a result of the March 2012 SPE period.

The GSFC 2-D model was used to predict medium-term impacts ($\sim$ months) from the

25   January and March 2012 SPE periods. Stratospheric ozone was most impacted in the polar SH by these solar events due to the increased downward motion in the months of March through November. These downward winds transported the SPE-produced $NO_y$ to lower altitudes and led to the destruction of ozone (up to 9 %) in the upper stratosphere. Total ozone reductions are predicted to be a maximum of $\sim$ 1 % in the SH

polar region during late winter and spring of 2012 due to the SPEs and would not likely be observed in total ozone satellite or ground measurements.

# References

Bernath, P. F., McElroy, C. T., Abrams, M. C., Boone, C. D., Butler, M., Camy-Peyret, C., Carleer, M., Clerbaux, C., Coheur, P.-F., Colin, R., DeCola, P., DeMazière, M., Drummond, J. R., Dufour, D., Evans, W. F. J., Fast, H., Fussen, D., Gilbert, K., Jennings, D. E., Llewellyn, E. J., Lowe, R. P., Mahieu, E., McConnell, J. C., McHugh, M., McLeod, S. D., Michaud, R., Midwinter, C., Nassar, R., Nichitiu, F., Nowlan, C., Rinsland, C. P., Rochon, Y. J., Rowlands, N., Semeniuk, K., Simon, P., Skelton, R., Sloan, J. J., Soucy, M.-A., Strong, K., Tremblay, P., Turnbull, D., Walker, K. A., Walkty, I., Wardle, D. A., Wehrle, V., Zander, R., and Zou, J.: Atmospheric Chemistry Experiment (ACE) mission overview, Geophys. Res. Lett., 32, L15S01, doi:10.1029/2005GL022386, 2005.

Considine, D. B., Douglass, A. R., and Jackman, C. H.: Effects of a polar stratospheric cloud parameterization on ozone depletion due to stratospheric aircraft in a two-dimensional model, J. Geophys. Res., 99, 18879–18894, 1994.

Damiani, A., Funke, B., Marsh, D. R., López-Puertas, M., Santee, M. L., Froidevaux, L., Wang, S., Jackman, C. H., von Clarmann, T., Gardini, A., Cordero, R. R., and Storini, M.: Impact of January 2005 solar proton events on chlorine species, Atmos. Chem. Phys., 12, 4159–4179, doi:10.5194/acp-12-4159-2012, 2012.

Douglass, A. R., Jackman, C. H., and Stolarski, R. S.: Comparison of model results transporting the odd nitrogen family with results transporting separate odd nitrogen species, J. Geophys. Res., 94, 9862–9872, 1989.

Fischer, H., Birk, M., Blom, C., Carli, B., Carlotti, M., von Clarmann, T., Delbouille, L., Dudhia, A., Ehhalt, D., Endemann, M., Flaud, J. M., Gessner, R., Kleinert, A., Koopman, R., Langen, J., López-Puertas, M., Mosner, P., Nett, H., Oelhaf, H., Perron, G., Remedios, J., Ridolfi, M., Stiller, G., and Zander, R.: MIPAS: an instrument for atmospheric and climate research, Atmos. Chem. Phys., 8, 2151–2188, doi:10.5194/acp-8-2151-2008, 2008.

Fleming, E. L., Jackman, C. H., Considine, D. B., and Stolarski, R. S.: Simulation of stratospheric tracers using an improved empirically based two-dimensional model transport formulation, J. Geophys. Res., 104, 23911–23934, 1999.

Fleming, E. L., Jackman, C. H., Weisenstein, D. K., and Ko, M. K. W.: The impact of interannual variability on multidecadal total ozone simulations, J. Geophys. Res., 112, D10310, doi:10.1029/2006JD007953, 2007.

Fleming, E. L., Jackman, C. H., Stolarski, R. S., and Douglass, A. R.: A model study of the impact of source gas changes on the stratosphere for 1850–2100, Atmos. Chem. Phys., 11, 8515–8541, doi:10.5194/acp-11-8515-2011, 2011.

Funke, B., Baumgaertner, A., Calisto, M., Egorova, T., Jackman, C. H., Kieser, J., Krivolutsky, A., López-Puertas, M., Marsh, D. R., Reddmann, T., Rozanov, E., Salmi, S.-M., Sinnhuber, M., Stiller, G. P., Verronen, P. T., Versick, S., von Clarmann, T., Vyushkova, T. Y., Wieters, N., and Wissing, J. M.: Composition changes after the "Halloween" solar proton event: the High Energy Particle Precipitation in the Atmosphere (HEPPA) model versus MIPAS data intercomparison study, Atmos. Chem. Phys., 11, 9089–9139, doi:10.5194/acp-11-9089-2011, 2011.

Heath, D. F., Krueger, A. J., and Crutzen, P. J.: Solar proton event: Influence on stratospheric ozone, Science, 197, 886–889, 1977.

Jackman, C. H., Frederick, J. E., and Stolarski, R. S.: Production of odd nitrogen in the stratosphere and mesosphere: An intercomparison of source strengths, J. Geophys. Res., 85, 7495–7505, 1980.

Jackman, C. H., Douglass, A. R., Rood, R. B., McPeters, R. D., and Meade, P. E.: Effect of Solar Proton Events on the Middle Atmosphere During the Past Two Solar Cycles as Computed Using a Two-dimensional Model, J. Geophys. Res., 95, 7417–7428, 1990.

Title Page

Abstract | Introduction

Conclusions | References

Tables | Figures

|◄ | ►|

◄ | ►

Back | Close

Full Screen / Esc

Printer-friendly Version

Interactive Discussion

Jackman, C. H., Fleming, E. L., Chandra, S., Considine, D. B., and Rosenfield, J. E.: Past, present, and future modeled ozone trends with comparisons to observed trends, J. Geophys. Res., 101, 28753–28767, 1996.

Jackman, C. H., McPeters, R. D., Labow, G. J., Fleming, E. L., Praderas, C. J., and Russell, J. M.: Northern hemisphere atmospheric effects due to the July 2000 solar proton event, Geophys. Res. Lett., 28, 2883–2886, 2001.

Jackman, C. H., DeLand, M. T., Labow, G. J., Fleming, E. L., Weisenstein, D. K., Ko, M. K. W., Sinnhuber, M., and Russell, J. M.: Neutral atmospheric influences of the solar proton events in October-November 2003, J. Geophys. Res., 100, A09S27, doi:10.1029/2004JA010888, 2005.

Jackman, C. H., Roble, R. G., and Fleming, E. L.: Mesospheric dynamical changes induced by the solar proton events in October–November 2003, Geophys. Res. Lett., 34, L04812, doi:10.1029/2006GL028328, 2007.

Jackman, C. H., Marsh, D. R., Vitt, F. M., Garcia, R. R., Fleming, E. L., Labow, G. J., Randall, C. E., López-Puertas, M., Funke, B., von Clarmann, T., and Stiller, G. P.: Short- and medium-term atmospheric constituent effects of very large solar proton events, Atmos. Chem. Phys., 8, 765–785, doi:10.5194/acp-8-765-2008, 2008.

Jackman, C. H., Marsh, D. R., Vitt, F. M., Garcia, R. R., Randall, C. E., Fleming, E. L., and Frith, S. M.: Long-term middle atmospheric influence of very large solar proton events, J. Geophys. Res., 114, D11304, doi:10.1029/2008JD011415, 2009.

Jackman, C. H., Marsh, D. R., Vitt, F. M., Roble, R. G., Randall, C. E., Bernath, P. F., Funke, B., López-Puertas, M., Versick, S., Stiller, G. P., Tylka, A. J., and Fleming, E. L.: Northern Hemisphere atmospheric influence of the solar proton events and ground level enhancement in January 2005, Atmos. Chem. Phys., 11, 6153–6166, doi:10.5194/acp-11-6153-2011, 2011.

Johnston, H. S. and Podolske, J.: Interpretations of stratospheric photochemistry, Rev. Geophys. Space Phys., 16, 491–519, 1978.

Krivolutsky, A. A., Klyuchnikova, A. V., Zakharov, G. R., Vyushkova, T. Y., and Kuminov, A. A.: Dynamical response of the middle atmosphere to solar proton event of July 2000: Three-dimensional model simulations, Adv. Space Res., 37, 1602–1613, 2006.

López-Puertas, M., Funke, B., Gil-López, S., von Clarmann, T., Stiller, G. P., Höpfner, M., Kellmann, S., Fischer, H., and Jackman, C. H.: Observation of NOx enhancement and ozone depletion in the Northern and Southern Hemispheres after the October–November 2003 solar proton events, J. Geophys. Res., 110, A09S43, doi:10.1029/2005JA011050, 2005a.

Title Page

Abstract | Introduction

Conclusions | References

Tables | Figures

|◄ | ►|

◄ | ►

Back | Close

Full Screen / Esc

Printer-friendly Version

Interactive Discussion

López-Puertas, M., Funke, B., Gil-López, S., von Clarmann, T., Stiller, G. P., Höpfner, M., Kellmann, S., Mengistu Tsidu, G., Fischer, H., and Jackman, C. H.: $HNO_3$, $N_2O_5$, and $ClONO_2$ enhancements after the October–November 2003 solar proton events, J. Geophys. Res., 110, A09S44, doi:10.1029/2005JA011051, 2005b.

5  McPeters, R. D. and Jackman, C. H.: The response of ozone to solar proton events during solar cycle 21: the observations, J. Geophys. Res., 90, 7945–7954, 1985.

Pickett, H. M., Read, W. G., Lee, K. K., and Yung, Y. L.: Observation of night OH in the mesosphere, Geophys. Res. Lett. 33, L19808, doi:10.1029/2006GL026910, 2006.

Porter, H. S., Jackman, C. H., and Green, A. E. S.: Efficiencies for production of atomic nitrogen
10  and oxygen by relativistic proton impact in air, J. Chem. Phys., 65, 154–167, 1976.

Randall, C. E., Siskind, D. E., and Bevilacqua, R. M.: Stratospheric NOx enhancements in the southern hemisphere vortex in winter/spring of 2000, Geophys. Res. Lett., 28, 2385–2388, 2001.

Rinsland, C. P., Boone, C., Nassar, R., Walker, K., Bernath, P., McConnell, J. C., and Chiou, L.:
15  Atmospheric Chemistry Experiment (ACE) Arctic stratospheric measurements of $NO_x$ during February and March 2004: Impact of intense solar flares, Geophys. Res. Lett., 32, L16S05, doi:10.1029/2005GL022425, 2005.

Sander, S. P., Friedl, R. R., Barker, J. R., Golden, D. M., Kurylo, M. J., Wine, P. H., Abbatt, J. P. D., Burkholder, J. B., Kolb, C. E., Moortgat, G. K., Huie, R. K., and Orkin, V. L.: Chemical
20  kinetics and photochemical data for use in atmospheric studies, Evaluation Number 17, JPL Publication 10-6, 2010.

Sinnhuber, M., Nieder, H., and Wieters, N.: Energetic particle precipitation and the chemistry of the mesosphere/lower thermosphere, Surv. Geophys., 33, 1281–1334, doi:10.1007/s10712-012-9201-3, 2012.

25  Solomon, S., Rusch, D. W., Gerard, J.-C., Reid, G. C., and Crutzen, P. J.: The effect of particle precipitation events on the neutral and ion chemistry of the middle atmosphere, 2, Odd hydrogen, Planet. Space Sci., 29, 885–892, 1981.

Solomon, S., Reid, G. C., Rusch, D. W., and Thomas, R. J.: Mesospheric ozone depletion during the solar proton event of July 13, 1982, 2, Comparison between theory and measurements,
30  Geophys. Res. Lett., 10, 257–260, 1983.

Swider, W. and Keneshea, T. J.: Decrease of ozone and atomic oxygen in the lower mesosphere during a PCA event, Planet. Space Sci., 21, 1969–1973, 1973.

**Atmospheric changes from solar proton events in 2012**

C. H. Jackman et al.

Title Page

| Abstract | Introduction |
| Conclusions | References |
| Tables | Figures |

|◀ | ▶|

◀ | ▶

Back | Close

Full Screen / Esc

Printer-friendly Version

Interactive Discussion

Verronen, P. T., Seppälä, A., Kyrola, E., Tamminen, J., Pickett, H. M., and Turunen, E.: Production of odd hydrogen in the mesosphere during the January 2005 solar proton event, Geophys. Res. Lett., 33, L24811, doi:10.1029/2006GL028115, 2006.

von Clarmann, T., Glatthor, N., Höpfner, M., Kellmann, S., Ruhnke, R., Stiller, G. P., Fischer, H., Funke, B., Gil-López, S., and López-Puertas, M.: Experimental evidence of perturbed odd hydrogen and chlorine chemistry after the October 2003 solar proton events, J. Geophys. Res., 110, A09S45, doi:10.1029/2005JA011053, 2005.

von Clarmann, T., Funke, B., López-Puertas, M., Kellmann, S., Linden, A., Stiller, G. P., Jackman, C. H., and Harvey, V. L.: The solar proton events in 2012 as observed by MIPAS, Geophys. Res. Lett., 40, 464–469, doi:10.1002/grl.50119, 2013.

WMO (World Meteorological Organization), Scientific Assessment of Ozone Depletion: 2010, Global Ozone Research and Monitoring Project-Report No. 52, Geneva, Switzerland, 2011.

Title Page

Abstract | Introduction

Conclusions | References

Tables | Figures

|◄ | ►|

◄ | ►

Back | Close

Full Screen / Esc

Printer-friendly Version

Interactive Discussion
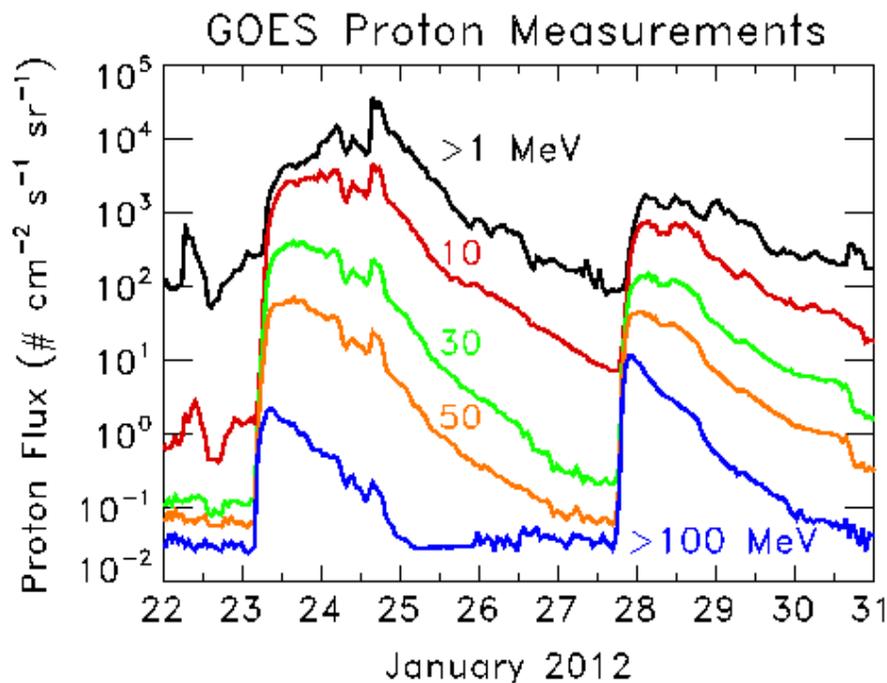
**Fig. 1.** GOES 13 proton flux measurements in January 2012 for energies $> 1\,\text{MeV}$ (black), $> 10\,\text{MeV}$ (red), $> 30\,\text{MeV}$ (green), $> 50\,\text{MeV}$ (gold), and $> 100\,\text{MeV}$ (blue). These data are provided by the NOAA SWPC at their website (see Sect. 2).

**Fig. 2.** Daily averaged ionization rates over the 10 to 0.001 hPa pressure range for the 22–30 January 2012 time period. Contour intervals are 100, 200, 500, 1000, and 2000 (#cm$^{-3}$ s$^{-1}$).

**Fig. 3.** GOES 13 proton flux measurements in March 2012 for energies > 1 MeV (black), > 10 MeV (red), > 30 MeV (green), > 50 MeV (gold), and > 100 MeV (blue). These data are provided by the NOAA SWPC at their website (see Sect. 2).

Title Page

Abstract | Introduction

Conclusions | References

Tables | Figures

|◄ | ►|

◄ | ►

Back | Close

Full Screen / Esc

Printer-friendly Version

Interactive Discussion
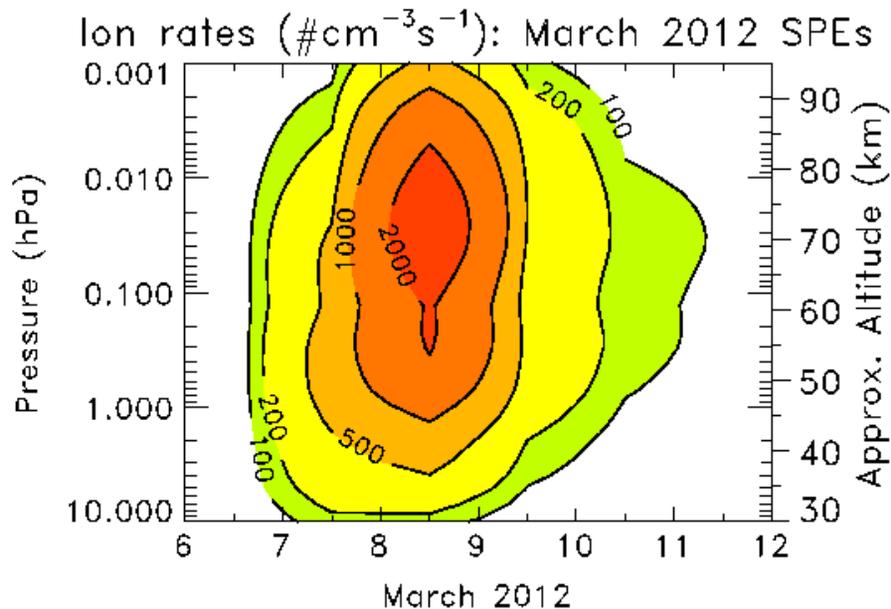
**Fig. 4.** Daily averaged ionization rates over the 10 to 0.001 hPa pressure range for the 6–11 March 2012 time period. Contour intervals are 100, 200, 500, 1000, and 2000 (#cm$^{-3}$ s$^{-1}$).

Title Page

Abstract | Introduction

Conclusions | References

Tables | Figures

|◄ | ►|

◄ | ►

Back | Close

Full Screen / Esc

Printer-friendly Version

Interactive Discussion
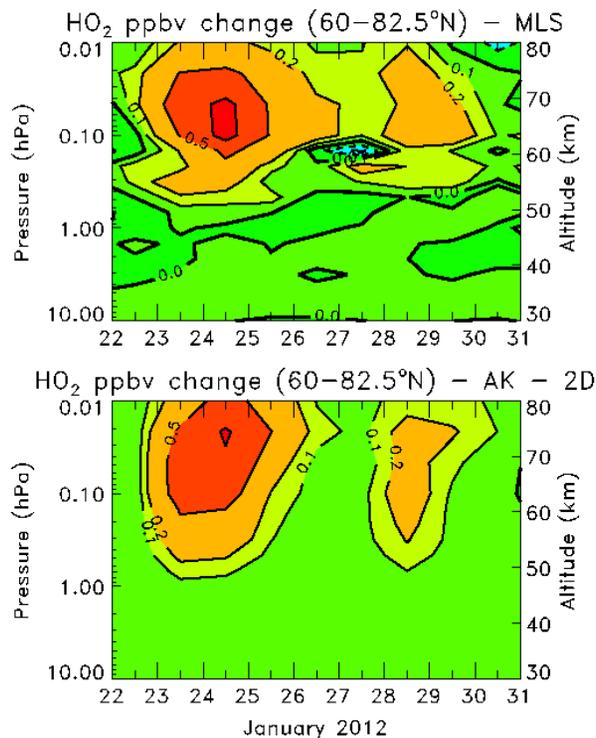
**Fig. 5.** Daily averaged $HO_2$ changes from Aura MLS measurements (Top) and GSFC 2-D model predictions (Bottom) for the 60–82.5° N band. An average observed (predicted) $HO_2$ profile for the period 18–22 January 2012 was subtracted from the observed (predicted) $HO_2$ values for the plotted days of 22–30 January 2012. The contour intervals for the $HO_2$ differences are −0.1, 0.0, 0.1, 0.2, 0.5, and 1 ppbv. The MLS averaging kernel (AK) was used to sample the model results.
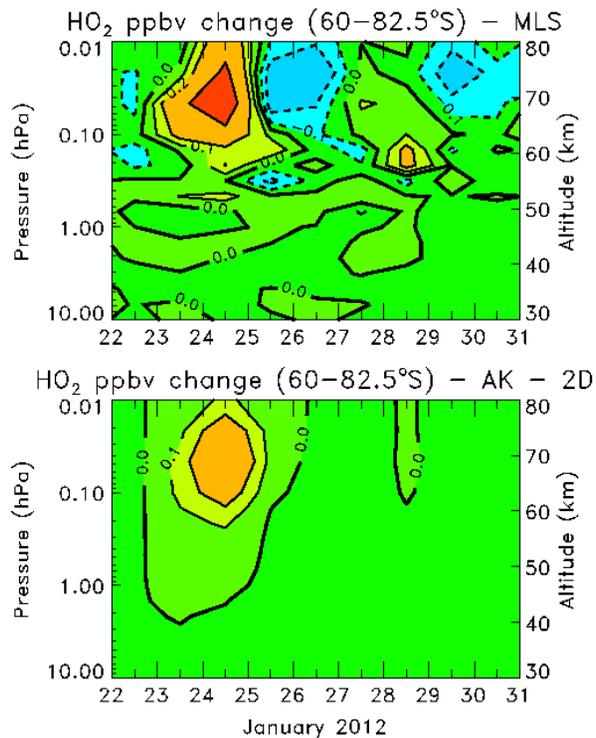
**Fig. 6.** Same as Fig. 5, but for the 60–82.5° S band. The contour intervals for the HO$_2$ differences are −0.2, −0.1, 0.0, 0.1, 0.2, 0.5, and 1 ppbv.
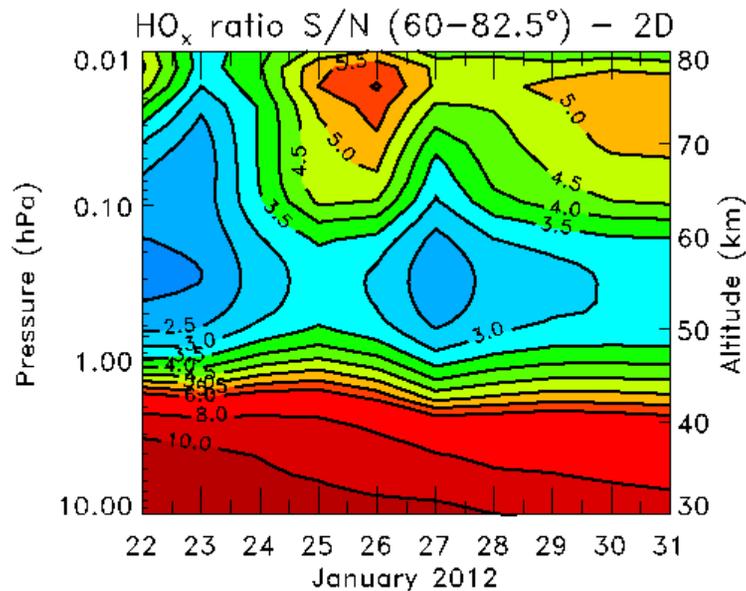
**Fig. 7.** Ratio of total HO$_x$ (H, OH, HO$_2$) concentration from the Southern (S) and Northern (N) Hemispheres for the 60–82.5° band from the GSFC 2-D model simulations. The contour intervals plotted are 2, 2.5, 3, 3.5, 4, 4.5, 5, 5.5, 6, 8, and 10.

Title Page

Abstract | Introduction

Conclusions | References

Tables | Figures

|◀ | ▶|

◀ | ▶

Back | Close

Full Screen / Esc

Printer-friendly Version

Interactive Discussion
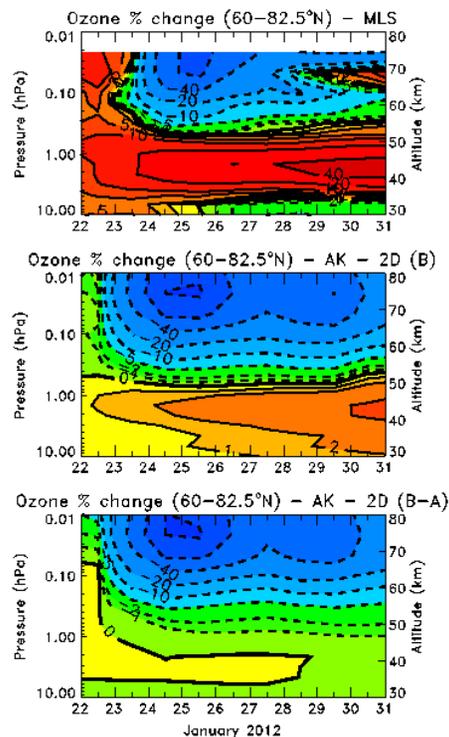
**Fig. 8.** Daily averaged ozone changes from Aura MLS measurements (Top) and GSFC 2-D model predictions (Middle, Bottom) for the 60–82.5° N band. An average observed (predicted) ozone profile for the period 18–22 January 2012 was subtracted from the observed (predicted) ozone values for the plotted days of 22–30 January 2012 for Aura MLS measurements (Top) and for the GSFC 2-D model simulation "B (with SPEs)" (Middle). The Bottom plot shows the difference between GSFC 2-D model simulations "B (with SPEs)" and "A (without SPEs)." The contour intervals for the ozone differences are −80, −60, −40, −20, −10, −5, −2, −1, 0, 1, 2, 5, 10, 20, and 40 %. The MLS averaging kernel (AK) was used to sample the model results.
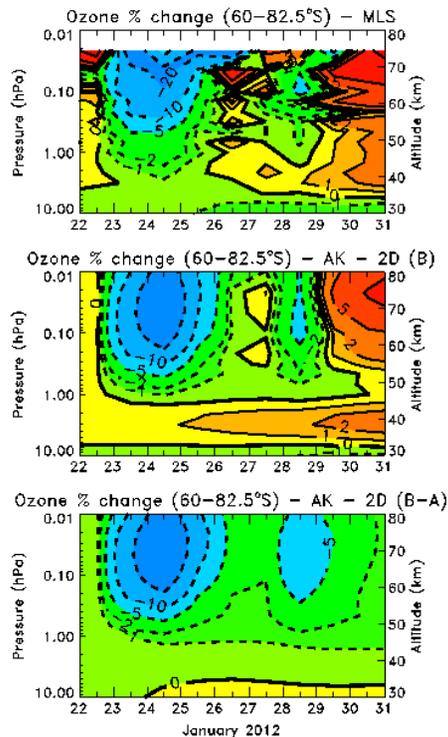
**Fig. 9.** Daily averaged ozone changes from Aura MLS measurements (Top) and GSFC 2-D model predictions (Middle, Bottom) for the 60–82.5° S band. An average observed (predicted) ozone profile for the period 18–22 January 2012 was subtracted from the observed (predicted) ozone values for the plotted days of 22–30 January 2012 for Aura MLS measurements (Top) and for the GSFC 2-D model simulation "B (with SPEs)" (Middle). The Bottom plot shows the difference between GSFC 2-D model simulations "B (with SPEs)" and "A (without SPEs)." The contour intervals for the ozone differences are −20, −10, −5, −2, −1, 0, 1, 2, 5, 10, and 20 %. The MLS averaging kernel (AK) was used to sample the model results.

Title Page

Abstract | Introduction

Conclusions | References

Tables | Figures

|◄ | ►|

◄ | ►

Back | Close

Full Screen / Esc

Printer-friendly Version

Interactive Discussion
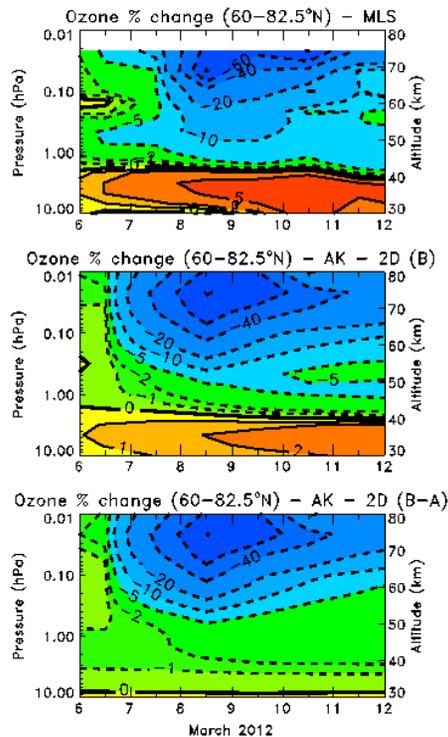
**Fig. 10.** Daily averaged ozone changes from Aura MLS measurements (Top) and GSFC 2-D model predictions (Middle, Bottom) for the 60–82.5° N band. An average observed (predicted) ozone profile for the period 2–6 March 2012 was subtracted from the observed (predicted) ozone values for the plotted days of 6–11 March 2012 for Aura MLS measurements (Top) and for the GSFC 2-D model simulation "B (with SPEs)" (Middle). The Bottom plot shows the difference between GSFC 2-D model simulations "B (with SPEs)" and "A (without SPEs)." The contour intervals for the ozone differences are −80, −60, −40, −20, −10, −5, −2, −1, 0, 1, 2, 5, and 10 %. The MLS averaging kernel (AK) was used to sample the model results.

Title Page

Abstract | Introduction

Conclusions | References

Tables | Figures

◄ | ►|

◄ | ►

Back | Close

Full Screen / Esc

Printer-friendly Version

Interactive Discussion
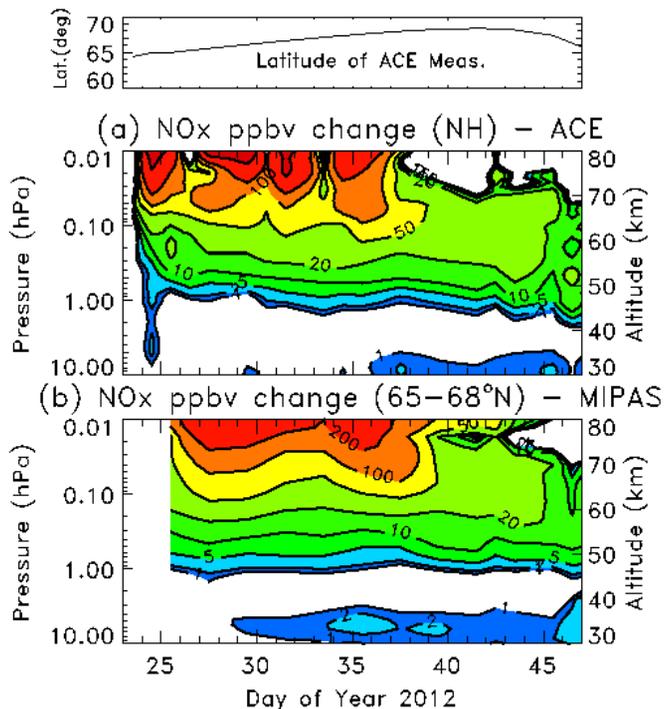
**Fig. 11.** Daily averaged NO$_x$ (NO+NO$_2$) changes from Day of Year (DoY) 22 (22 January) 2012 values as measured by ACE **(a)** and MIPAS (65–68° N) **(b)**. The contour intervals for the NO$_x$ differences are 1, 2, 5, 10, 20, 50, 100, 200, and 500 ppbv. The Northern polar latitudes of ACE measurements are given in the Top plot.

**Fig. 12.** Daily averaged $NO_x$ (NO+$NO_2$) changes from DoY 22 (22 January) 2012 values for 60–90° N as measured by MIPAS (Top) and calculated by the GSFC 2-D model (Bottom). The contour intervals for the $NO_x$ differences are 1, 2, 5, 10, 20, 50, 100, 200, and 500 ppbv.

**Fig. 13.** Daily averaged NO$_x$ (NO+NO$_2$) changes from DoY 22 (22 January) 2012 values for 60–90° S as measured by MIPAS (Top) and calculated by the GSFC 2-D model (Bottom). The contour intervals for the NO$_x$ differences are 1, 2, 5, 10, 20, 50, and 100 ppbv.

Discussion Paper | Discussion Paper | Discussion Paper | Discussion Paper |

**ACPD**

13, 23251–23293, 2013

**Atmospheric changes from solar proton events in 2012**

C. H. Jackman et al.

Title Page

Abstract | Introduction

Conclusions | References

Tables | Figures

|◄ | ►|

◄ | ►

Back | Close

Full Screen / Esc

Printer-friendly Version

Interactive Discussion

**Fig. 14.** Daily averaged NO$_x$ (NO+NO$_2$) changes from DoY 66 (6 March) 2012 values as measured by ACE **(a)** and MIPAS (78-83° N) **(b)**. The contour intervals for the NO$_x$ differences are 1, 2, 5, 10, 20, 50, and 100 ppbv. The Northern polar latitudes of ACE measurements are given in the Top plot.

Title Page

Abstract | Introduction

Conclusions | References

Tables | Figures

|◀ | ▶|

◀ | ▶

Back | Close

Full Screen / Esc

Printer-friendly Version

Interactive Discussion
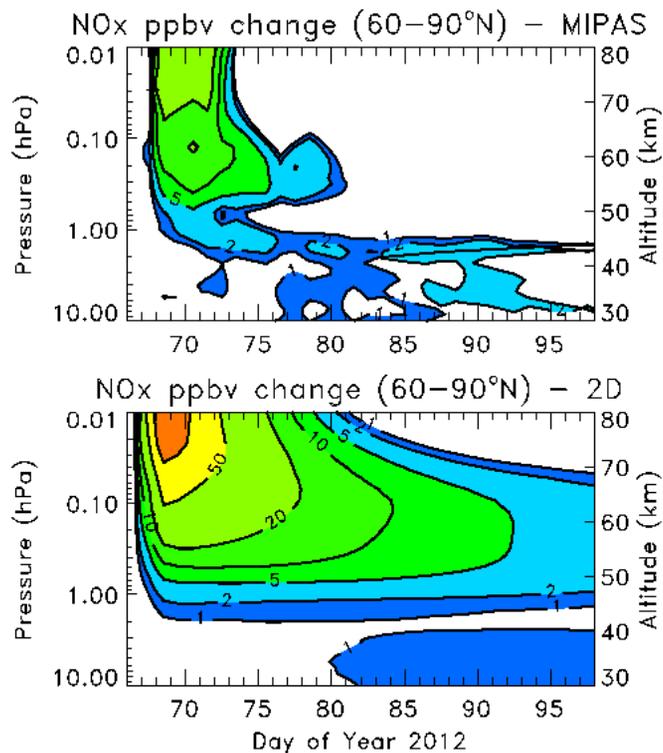
**Fig. 15.** Daily averaged $NO_x$ (NO + $NO_2$) changes from DoY 66 (6 March) 2012 values for 60–90° N as measured by MIPAS (Top) and calculated by the GSFC 2-D model (Bottom). The contour intervals for the $NO_x$ differences are 1, 2, 5, 10, 20, 50, and 100 ppbv.

## ACPD

13, 23251–23293, 2013

**Atmospheric changes from solar proton events in 2012**

C. H. Jackman et al.

Title Page

Abstract     Introduction

Conclusions     References

Tables     Figures

◄     ►|

◄     ►

Back     Close

Full Screen / Esc

Printer-friendly Version

Interactive Discussion

**Fig. 16.** Daily averaged $NO_x$ ($NO+NO_2$) changes from the DoY 66 (6 March) 2012 values for 60–90° S as measured by MIPAS (Top) and calculated by the GSFC 2-D model (Bottom). The contour intervals for the $NO_x$ differences are 1, 2, 5, 10, 20, 50, and 100 ppbv.
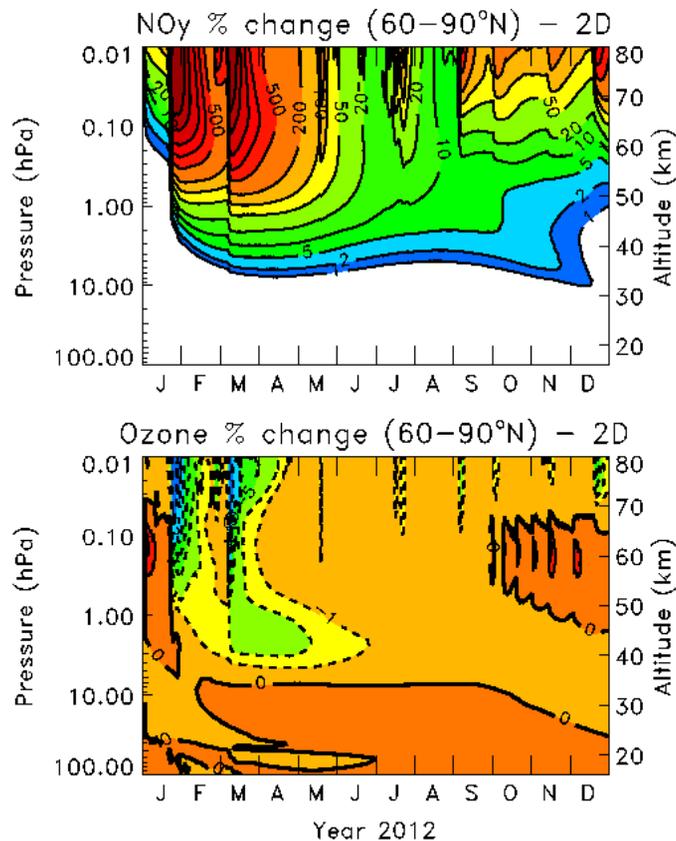
**Fig. 17.** Difference between GSFC 2-D model simulation "B (with SPEs)" and "A (without SPEs)" for NO$_y$ (*Top*) and Ozone (Bottom) for 60–90° N for all months of 2012. The contour intervals for the NO$_y$ differences are 1, 2, 5, 10, 20, 50, 100, 200, 500, 1000, 2000, 5000, and 10 000 % (Top). The contour intervals for the Ozone differences are −50, −20, −10, −5, −2, −1, 0, 1, and 2 % (Bottom).

Title Page

Abstract | Introduction

Conclusions | References

Tables | Figures

|◄ | ►|

◄ | ►

Back | Close

Full Screen / Esc

Printer-friendly Version

Interactive Discussion
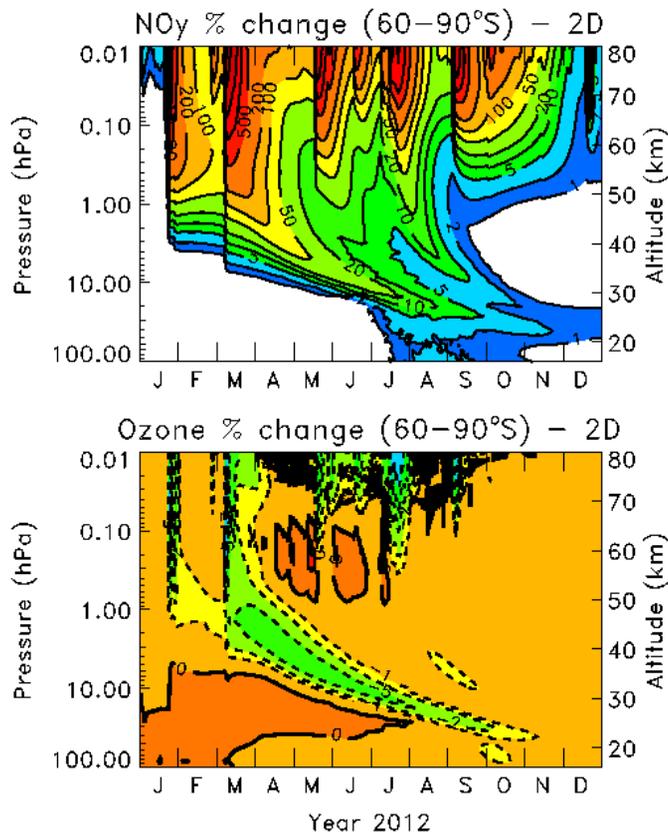
**Fig. 18.** Difference between GSFC 2-D model simulation "B (with SPEs)" and "A (without SPEs)" for NO$_y$ (Top) and Ozone (Bottom) for 60–90°S for all months of 2012. The contour intervals for the NO$_y$ differences are 1, 2, 5, 10, 20, 50, 100, 200, 500, 1000, 2000, and 5000 % (Top). The contour intervals for the Ozone differences are −50, −20, −10, −5, −2, −1, 0, and 1 % (Bottom).

Title Page

Abstract | Introduction

Conclusions | References

Tables | Figures

|◄ | ►|

◄ | ►

Back | Close

Full Screen / Esc

Printer-friendly Version

Interactive Discussion
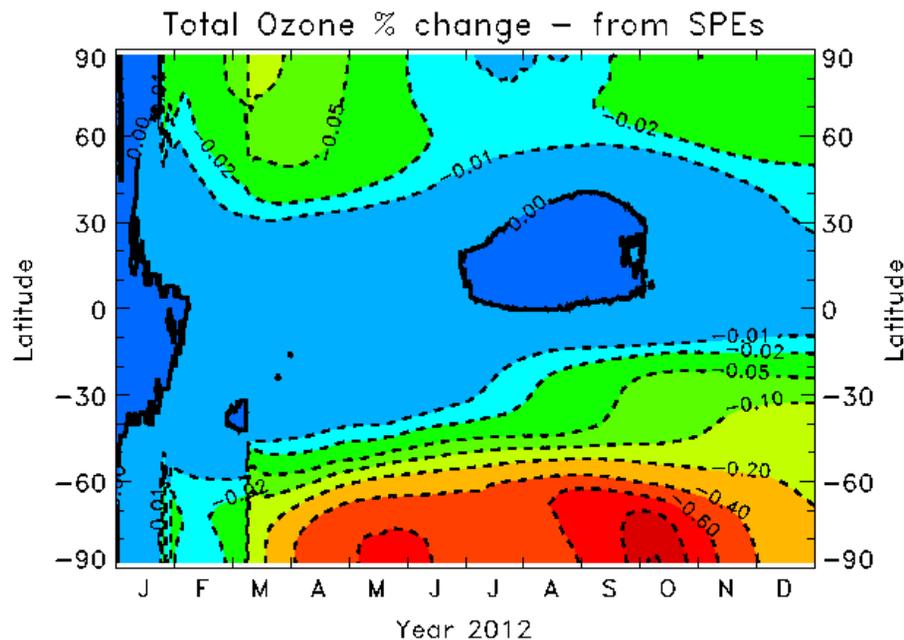
**Fig. 19.** Difference between GSFC 2-D model simulation "B (with SPEs)" and "A (without SPEs)" for total ozone for all months of 2012 at all latitudes. The contour intervals are −1, −0.8, −0.6, −0.4, −0.2, −0.1, −0.05, −0.02, −0.01, and 0 %.

Full Screen / Esc

Printer-friendly Version

Interactive Discussion